Mechanistic Studies of the 5-Iodouracil Chromophore Relevant to Its Use in Nucleoprotein Photo-Cross-Linking

Christopher L. Norris, Poncho L. Meisenheimer, and Tad H. Koch*

Contribution from the Department of Chemistry and Biochemistry, University of Colorado, Boulder, Colorado 80309-0215

Received March 11, 1996[⊗]

Abstract: The photoreactivity of the 5-iodouracil chromophore was investigated toward understanding photo-cross-linking of nucleic acids bearing the chromophore to functionality in associated proteins. Irradiation of 5-iodouridine (IU) in the presence of a 10-fold excess of *N*-acetyltyrosine *N*-ethylamide (**1**) at 308 nm with a XeCl excimer laser or at 325 nm with a HeCd laser yields uridine (U) and *N*-acetyl-*m*-(5-uridinyl)tyrosine *N*-ethylamide (**2**) in a 1:2 mole ratio. In the presence of *N*-acetylphenylalanine *N*-ethylamide, uridine and analogous ortho, meta, and para regioisomeric adducts (**3o**, **3m**, and **3p**) were formed in a similar U to adduct mole ratio. The primary photochemical process leading to products was established as carbon−iodine bond homolysis in the first excited singlet state from a deuterium labeling experiment, photoacoustic calorimetry, and quantum yield measurements. Photoreduction of IU in 2-propanol-*d* solvent gave U with no deuterium incorporation. Photoacoustic calorimetric measurements established that triplet benzophenone transferred energy to IU with a rate constant of 2×10^9 M^{-1} s^{-1}. Further, the reaction of IU with **1** to form **2** was sensitized by benzophenone; however, comparison of quantum yields upon direct and sensitized excitation indicated that, at most, only a small portion of the reactions occurred via the triplet state. With direct excitation of IU, quantum yields as a function of the concentration of **1** showed that U and adduct **2** resulted from a common intermediate proposed to be the 5-uridinyl radical. Uridine formation was enhanced by the presence of hydrogen atom donors at the expense of formation of **2**. Quantum yields were independent of excitation wavelength in the region 310−330 nm but not the reaction medium. The quantum yield of uridine formation but not adduct formation was approximately an order of magnitude higher in 90% acetonitrile−10% water than in pH 7 water. The results are discussed in terms of high-yield cross-linking of nucleic acids bearing the 5-iodouracil chromophore to associated proteins in light of cocrystal X-ray structural data.

Introduction

Photo-cross-linking is an established technique for identifying regions of nucleoprotein complexes which are in proximity.[1−5] It can also have potential for locating an unknown protein for which binding to a known nucleic acid sequence is proposed to have biological significance. The information content of the photo-cross-linking experiment, however, is dependent upon the specificity of the photoreaction, the level of perturbation of the complex caused by introduction of molecular changes needed to achieve photo-cross-linking, and the potential for identification of the cross-link position. A major problem associated with utilizing the technique has been the cross-linking yield. When the yield is only a few percent, the specificity is in question. Did the cross-linking result from a nonspecific encounter of the partners of the complex? Photodamage to other sites within the nucleoprotein complex can also be competitive and affect subsequent photo-cross-linking and/or sequencing.

Three studies now indicate that 5-iodouracil is an excellent chromophore for introduction into both RNA and DNA for the purpose of achieving specific photo-cross-linking to associated protein and that it can be superior to its predecessor, 5-bromouracil, in this application. In RNA, 5-iodouracil replaces uracil and in DNA, thymine, and consequently, the substitution produces minimal spatial perturbation of the nucleoprotein complex of interest, especially with DNA. The three nucleoprotein complexes which have been characterized using the technique are a variant of a small RNA hairpin loop within the genome of the bacteriophage R17 bound to the R17 coat protein,[2] the single-stranded DNA telomeric sequence of the ciliated protozoan, *Oxytricha nova*, bound to its telomere binding protein,[3] and a variant of a stem loop of the U1 snRNA bound to the N-terminal RNA binding domain of human U1A snRNP protein.[4] Sequencing has established cross-linking to specific tyrosine,[2,3,5] histidine,[2,3] and phenylalanine[4] residues. In all three systems the cross-linking yield with 5-iodouracil substitution was 3−5 times higher than with corresponding 5-bromouracil substitution.

A new application of nucleoprotein photo-cross-linking, which depends in a very significant way on the cross-linking yield, is photoSELEX. PhotoSELEX is a methodology for identification of a nucleic acid, bearing one or more photoreactive nucleotides, from a large combinatorial library which will bind with high affinity to a target protein and photo-cross-link to the target protein in high yield. The methodology is based upon the SELEX protocol, selective evolution of ligands by exponential enrichment.[6] A successful photoselection was recently demonstrated with the iodouracil chromophore and HIV-1 Rev as the target protein.[7]

[⊗] Abstract published in *Advance ACS Abstracts,* June 1, 1996.

(1) Budowsky, E. I.; Abdurashidova, G. G. *Prog. Nucl. Res.* **1989**, *37*, 1. Abdurashidova, G. G.; Tsvetkova, E. A.; Budowsky, E. I. *Nucl. Acids Res.* **1991**, *19*, 1909. Allen, T. D.; Wick, K. L.; Matthews, K. S. *J. Biol. Chem.* **1991**, *266*, 6113. Wower, J.; Hixson, S. S.; Zimmermann, R. A. *Biochemistry* **1988**, *27*, 8114. Lee, D. K.; Evans, R. K.; Blanco, J.; Gottesfeld, J.; Johnson, J. D. *J. Biol. Chem.* **1991**, *266*, 16478. Sontheimer, E. J. *Mol. Biol. Rep.* **1994**, *20*, 35.

(2) Willis, M. C.; Hicke, B. J.; Uhlenbeck, O. C.; Cech, T. R.; Koch, T. H. *Science* **1993**, *262*, 1255.

(3) Hicke, B. J.; Willis, M. C.; Koch, T. H.; Cech, T. R. *Biochemistry* **1994**, *33*, 3364.

(4) Stump, W. T.; Hall, K. B. *RNA* **1995**, *1*, 55.

(5) Willis, M. C.; LeCuyer, K. A.; Meisenheimer, K. M.; Uhlenbeck, O. C.; Koch, T. H. *Nucleic Acids Res.* **1994**, *22*, 4947.

(6) Turek, C.; Gold, L. *Science* **1990**, *249*, 505.

S0002-7863(96)00785-8 CCC: $12.00

Earlier mechanistic studies of the 5-bromouracil chromophore revealed two primary photochemical processes with potential for photo-cross-linking, carbon−bromine bond homolysis and photoelectron transfer.[8,9] Further, partitioning between the two processes was excitation wavelength dependent.[10] Signatures for the two processes were respective deuterium incorporation in the product uracil upon irradiation in variously-deuterium-labeled 2-propanol. With 2-propanol-*d* solvent, 5-deuteriouracil formation was the signature for electron transfer, and uracil formation for bond homolysis; with 2-deuterio-2-propanol solvent the signatures were reversed. Irradiation of 5-bromouracil at 254 nm in 2-propanol-*d* solvent gave approximately two-thirds uracil and one-third 5-deuteriouracil; irradiation at 308 nm with a XeCl excimer laser gave predominantly 5-deuteriouracil. Further, deuterium incorporation with 2-propanol-*d* solvent was quenched by *cis*-piperylene. These and other observations were interpreted in terms of bond homolysis in the higher energy π,π^* singlet state, little or no bond homolysis in the lower energy n,π^* singlet state, and intersystem crossing from both singlet states to the triplet state which reacts by electron transfer.

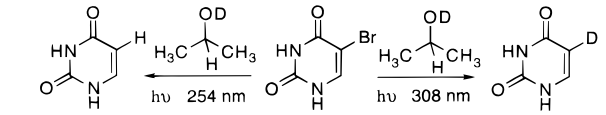

We perceived photoelectron transfer to be the more desirable mechanism for achieving high-specificity photo-cross-linking of nucleoprotein complexes because reactivity should depend upon the proximity of the halouracil to electron rich functionality in the protein. Bond homolysis should not depend upon the environment and has potential for promiscuity. Fortuitously, the photoelectron transfer mechanism can be selected with excitation at longer wavelengths. Model studies established cross-linking of bromouracil to derivatives of tyrosine, histidine, tryptophan,[11] and cystine[12] upon 308 nm excitation. Further, improved yields of nucleoprotein cross-linking with the 5-bromouracil chromophore have been achieved with 308 nm excitation.[13]

A recent mechanistic study of the photoreaction between 5-bromouridine and *N*-acetyltyrosine *N*-ethylamide to produce an adduct as well as uridine points to a further variation on photoelectron transfer initiation of cross-linking.[14] Quantum yield measurements together with careful UV absorption measurements suggested that the majority of product formation resulted from excited tyrosine donating an electron to bromouridine rather than excited bromouridine abstracting an electron from the ground state tyrosine derivative. Presumably, this mechanism extends to the tryptophan chromophore but not to the histidine chromophore which is transparent except at wavelengths below 250 nm.

The high nucleoprotein photo-cross-linking yields achieved with 5-iodouracil substituted nucleic acids suggested that the primary photochemical process with excitation at the long-wavelength tail of the absorption band was also photoelectron transfer, possibly with the 5-iodouracil chromophore in the triplet state. However, a number of studies with 5-iodouracil,[14−16] 5-iodouridine,[17] and even oligonucleotides[18] and nucleic acids[19,20] bearing 5-iodouracil have concluded that the primary photochemical process of this chromophore is carbon−iodine bond homolysis. Indeed, carbon−iodine bond homolysis is a general photoreaction of organic iodides,[21,22] including vinyl iodides.[23] Because of the emerging importance of the 5-iodouracil chromophore in the characterization of nucleoprotein complexes and photoSELEX and a perceived inconsistency of the accepted carbon−iodine bond homolysis mechanism with high-yield photo-cross-linking, we reinvestigated the photoreactivity, focusing on the primary photochemical process or processes leading to photo-cross-linking. We now describe the results of time-resolved photoacoustic calorimetric measurements, photoreduction in 2-propanol-*d* solvent, and quantum yield measurements of photoreaction in the presence of a tyrosine derivative.

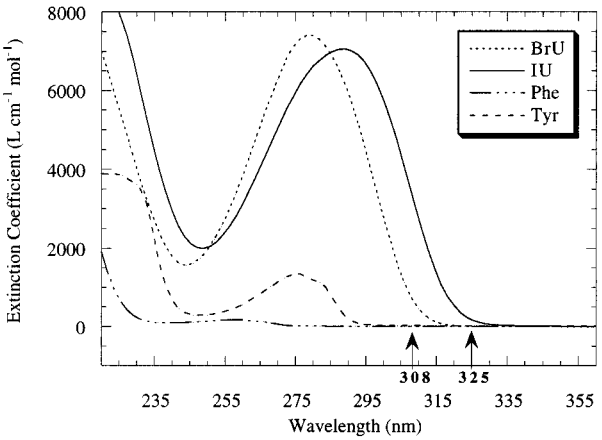

Figure 1. Comparison of UV absorption by 5-bromouridine (···), 5-iodouridine (—), *N*-acetylphenylalanine *N*-ethylamide (—···—), and *N*-acetyltyrosine *N*-ethylamide (- - -) in 20 mM, pH 7 phosphate buffer.

Results and Discussion

Absorption and Emission. The UV absorption by IU is compared with absorption by 5-bromouridine (BrU) and derivatives of the amino acids tyrosine and phenylalanine in Figure 1 in pH 7 buffered water. Of particular importance are absorptions in the region 300−330 nm. 5-Iodouridine absorbs more intensely in this region than BrU or any of the wild-type nucleosides or amino acid residues with a molar extinction coefficient of 165 L mol^{-1} cm^{-1} at 325 nm. This is particularly significant because monochromatic 325 nm light is available at reasonable intensity and cost from a helium−cadmium

(7) Jensen, K. B.; Atkinson, B. L.; Willis, M. C., Koch, T. H.; Gold, L. *Proc. Natl. Acad. Sci. U.S.A.* **1995**, *92*, 12220.
(8) Ito, S.; Saito, I.; Matsuura, T. *J. Am. Chem. Soc.* **1980**, *102*, 7535.
(9) Swanson, B. J.; Kutzer, J. C.; Koch, T. H. *J. Am. Chem. Soc.* **1981**, *103*, 1274.
(10) Dietz, T. M.; Trebra, R. J. von; Swanson, B. J.; Koch, T. H. *J. Am. Chem. Soc.* **1987**, *109*, 1793.
(11) Dietz, T. M.; Koch, T. H. *Photochem. Photobiol.* **1987**, *46*, 971.
(12) Dietz, T. M.; Koch, T. H. *Photochem. Photobiol.* **1989**, *49*, 121.
(13) Gott, J. M.; M. C, W.; Koch, T. H.; Uhlenbeck, O. C. *Biochemistry* **1991**, *30*, 6290.
(14) Norris, C.; Meisenheimer, K. M.; Koch, T. H. *Photochem. Photobiol.* **1996**, submitted.
(15) Rupp, W. D.; Prusoff, W. H. *Biochem. Biophys. Res. Commun.* **1965**, *18*, 158.
(16) Gilbert, E.; Schulte-Frohlinde, D. *Z. Naturforsch., Teil B*, **1970**, *25*, 492. Gilbert, E.; Wagner, G.; Schulte-Frohlinde, D. *Z. Naturforsch., Teil B*, **1971**, *26*, 209. Gilbert, E.; Wagner, G.; Schulte-Frohlinde, D. *Z. Naturforsch., Teil B*, **1972**, *27*, 501.
(17) Görner, H. *J. Photochem. Photobiol., A* **1993**, *72*, 197.
(18) Sugiyama, H.; Tsutsumi, Y.; Fujimoto, K.; Saito, I. *J. Am. Chem. Soc.* **1993**, *115*, 4443.
(19) Rahn, R. O.; Sellin, H. G. *Photochem. Photobiol.* **1983**, *37*, 661.
(20) Wood, T. G.; Marongiu, M. E.; Prusoff, W. H. *Biochem. Pharmacol.* **1991**, *41*, 439.
(21) Kropp, P. J.; Worsham, P. R.; Davidson, R. I.; Jones, T. H. *J. Am. Chem. Soc.* **1982**, *104*, 3972.
(22) Slocum, G. H.; Kaufmann, K.; Schuster, G. B. *J. Am. Chem. Soc.* **1981**, *103*, 4625.
(23) Kropp, P. J.; NcNeely, S. A.; Davis, R. D. *J. Am. Chem. Soc.* **1983**, *105*, 6907.

(HeCd) laser. 5-Iodouridine in pH 7 buffered water showed little or no fluorescence. A measurement of the fluorescence quantum yield placed an upper limit on the quantum yield at 1×10^{-3}, suggesting a short singlet lifetime.

Photoreactions. Irradiation of IU at 308 nm with a xenon chloride (XeCl) excimer laser or at 325 nm with a HeCd laser in the presence of an excess of *N*-acetyltyrosine *N*-ethylamide (**1**) in pH 7 aqueous medium yielded primarily uridine and *N*-acetyl-*m*-(5-uridinyl)tyrosine *N*-ethylamide (**2**) in a 1:2 mole ratio. The reaction was carried only to 50% destruction of IU because **2** was somewhat photolabile with irradiation in the region 300−330 nm. Adduct **2** was isolated by preparative reversed phase HPLC and characterized from spectroscopic data as reported in the Experimental Section and Table 1. The assignment of the ^{1}H NMR signals was made from splitting patterns and homonuclear COSY spectra. NOE difference spectroscopy established the regioconnectivity of the cross-link between the 5-position of iodouridine and the meta position of the tyrosine analog. Adduct **2** was identical to the adduct from irradiation of a pH 7 solution of 5-bromouridine and **1**.[14]

Similar irradiation of IU in the presence of an excess of *N*-acetylphenylalanine *N*-ethylamide at 308 nm gave uridine (30%) and three regioisomeric adducts, *N*-acetyl-*o*-(5-uridinyl)-phenylalanine *N*-ethylamide (**3o**), *N*-acetyl-*m*-(5-uridinyl)phenylalanine *N*-ethylamide (**3m**), and *N*-acetyl-*p*-(5-uridinyl)phenylalanine *N*-ethylamide (**3p**) in the ratio 1:2:1 (65% total yield by HPLC). The para isomer was separated from the ortho and meta isomers by preparative reversed phase HPLC, and all three isomers were characterized from ^{1}H NMR and mass spectral data reported in Table 1 and the Experimental Section.

Irradiation at 308 nm of IU in 2-propanol-*d* solvent to 50% destruction gave uridine as the sole product. Isolation of the uridine and characterization by ^{1}H NMR spectroscopy showed no deuterium incorporation at the 5-position. In contrast, an analogous experiment with 5-bromouracil gave uracil with approximately 80% deuterium incorporation at the 5-position.[9] This result is consistent with carbon−iodine bond homolysis in contrast with electron transfer as the primary photochemical process.

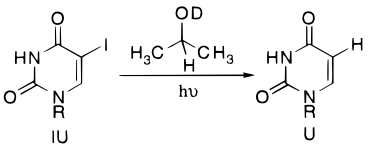

Photoacoustic Calorimetry. Irradiation of 5-iodouridine in a 90:10 acetonitrile−water mixture (v/v) gave rise to an enthalpy release shortfall versus the calibrant of 9 ± 3% in argon-saturated solution with excitation at 310 nm. Thus, a small but significant fraction of the originally-absorbed photon energy was retained in the form of endothermic products on a time scale longer than the maximum kinetic lifetime detectable by the apparatus (about 5 μs). No evidence of kinetic events within the 200 ns to 5 μs lifetime resolution window was found. In buffered aqueous solution, however, no statistically significant enthalpic shortfall was detected, assuming that all of the photoacoustic signal that arises is truly enthalpic in origin. Irradiation in the presence of the tyrosine derivative did nothing to change this observation. The effect of the medium on photoreactivity was also apparent from quantum yield measurements (vide infra).

Photoacoustic calorimetry was also used to study the triplet state of 5-iodouridine produced by benzophenone sensitization in 90:10 acetonitrile−water. Higher IU concentrations resulted in more prompt heat deposition, which shifted the phases of the acoustic waves to match more closely that of the calibrant; the calibrant deposited all of its photon energy on a time scale faster than the apparatus could respond to it. Rate constant fits to the photoacoustic waves gave data for a Stern−Volmer plot for iodouracil quenching of benzophenone. The plot was linear with a slope, $(1.88 \pm 0.03) \times 10^9$ M^{-1} s^{-1}, equal to the rate constant for energy transfer. The photoacoustic experiment also provided a measure of the benzophenone triplet energy, 68.4 ± 0.6; agreement with the literature value of 69 kcal/mol provided an internal check of the experiment. The rate constant for energy transfer to IU is about an order of magnitude below the rate constant for diffusion in acetonitrile, consistent with a triplet state energy close to that of benzophenone. This estimate is in agreement with one made some years ago from phosphorescence excitation spectra in the solid state.[24] As expected the triplet energy is below that of 5-bromouracil which has been estimated at about 72 kcal/mol.[17,24] Further, the photoacoustic measurements indicate that no enthalpic shortfall or excess is observed in the total amount of heat released. Thus, the excited triplet state of 5-iodouracil undergoes no photochemistry aside from direct relaxation to ground state iodouracil. An alternative, albeit unlikely, possibility (vide infra) is that triplet IU undergoes photochemistry to thermoneutral products on a time scale faster than the minimum time resolution of the photoacoustic technique, which in this case is 200 ns.

Quantum Yield Measurements. Direct irradiation of 1 mM 5-iodouridine with 8 mM *N*-acetyltyrosine *N*-ethylamide in buffered pH 7 aqueous solution at 325 nm with a HeCd laser gave uridine (U) and *N*-acetyl-*m*-(5-uridinyl)tyrosine *N*-ethylamide (**2**) with quantum yields of destruction and formation as shown in Table 2 (entry 1). The quantum yield of destruction and the sum of the quantum yields of formation were in the range of 1.5%; the low quantum yields are consistent with the lack of an observable enthalpic shortfall in the photoacoustic experiment in this medium. Direct irradiation of 5-iodouridine alone gave rise to a similar, if not slightly greater, iodouridine destruction quantum yield (Table 3, entry 1). Most but not all of this destruction was accounted for by uridine formation, with many other products present in the HPLC chromatograms. The effect of the concentration of the tyrosine derivative **1** on the partitioning between uridine formation and adduct **2** formation is shown in Figure 2. At concentrations of **1** above 10 mM, the product ratio (1:2) does not change and quantum yields become constant. Hence, at higher concentrations of **1**, reduction and adduct formation are coupled and result from reaction of a common intermediate, such as the uridinyl radical, with **1**. Further, at concentrations of the reactants employed, the common intermediate must not be able to re-form significant amounts of starting material.

Irradiation of IU and **1** in a 90:10 (v/v) acetonitrile−water mixture gave rise to a similar quantum yield of adduct formation but an unexpectedly high quantum yield of reduction to U as reported in Table 3 (entry 6). The uridine to adduct **2** ratio was almost 10:1, and the IU destruction quantum yield was about a factor of 10 greater than that in aqueous solution. In this experiment the analysis for U was complicated by the presence of acetonitrile in the HPLC injection solvent which caused significant broadening of the uridine peak. Identification of the broad peak as U was established by comparison with the peak from injection of a sample of U in 90:10 acetonitrile−water. The assumption that the integral of this broad peak between 0.5 and 2 min was a measure of uridine formation was supported by a resulting destruction quantum yield approximately equal to the product formation quantum yield. The

(24) Rothman, W.; Kearns, D. R. *Photochem. Photobiol.* **1967**, *6*, 775.

Table 1. 400 MHz ^{1}H NMR Data

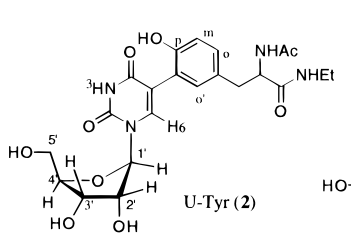

U-Tyr (**2**)

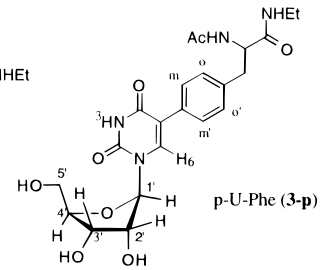

p-U-Phe (**3-p**)

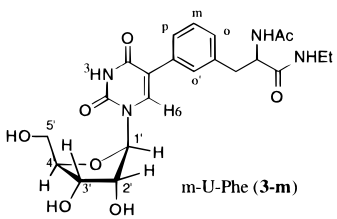

m-U-Phe (**3-m**)

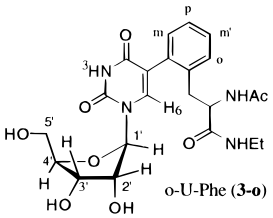

o-U-Phe (**3-o**)

compound	position													
	NHAc	NHEt	α	*β*	*o*,*o*′	*m*,*m*′	*p*	3	6	1′	2′	3′	4′	5′
U-Tyr (**2**) (DMSO-d_6)	1.76, s 7.99, d, $J = 8$[h]	0.93, t, $J = 7$ 3.02, dq, $J = 6, 7$ 7.90, t, $J = 6$	4.33, ddd, $J = 5, 8, 9$	2.62, dd, $J = 9, 14$ 2.80, dd, $J = 5, 14$	6.97, d, $J = 8$ 6.98, s	6.70, d, $J = 8$	9.25, br s	9.50, br s	7.90, s	5.83, d, $J = 5$	4.06, ∼q,[a] $J \approx 5$ 5.41, OH, d, $J = 5$	3.95, ∼q,[a] $J \approx 5$ 5.10, OH, d, $J = 5$	3.84,[b] ∼q,[a] $J \approx 5$	3.51[c] 3.58,[d] $J_{ab} = 14$, $J_{ax} \approx J_{am}$, $J_{ax} \approx 5$ 4.98,[e] OH, t, $J = 5$
p-U-Phe[f] (**3p**) (DMSO-d_6 −D_2O)	1.76, s	0.94, t, $J = 7$ 3.04, dq, $J = 6, 7$ 8.13, t, $J = 6$	4.41, m	2.74, dd 2.91, dd	7.44, d, $J = 8$	7.19, d, $J = 8$			7.99, s	5.83, d	4.05, m	3.65, m	3.59, m	4.13, m 4.18, m
m-U-Phe[f] (**3m**) (DMSO-d_6 −D_2O)	1.69, s	0.85, t, $J = 7$ 2.95, q, $J = 7$	4.43, m	2.69, m 2.75, m	7.21, d 7.33, s	7.26, m	7.05, d, $J = 8$		7.88, s	5.81, d	3.87, dd	3.58, dd	3.49, m	4.05, m 4.10, m
o-U-Phe[f] (**3o**) (DMSO-d_6 −D_2O)	1.78, s	0.83, t, $J = 7$ 2.92, q, $J = 7$	4.41, m	2.6, m 2.7, m	7.19, d	7.14, d, $J = 8$ 7.23, m	7.24, m		8.21, s	5.80, d	3.82, dd	3.67, dd	3.58, m	4.05, m 4.10, m

[a] The ribose hydrogens appear as quartets due to similar coupling with the three nonequivalent neighbors. [b] X of the ABMX pattern with further coupling to the proton at 3′. [c] A of ABMX. [d] B of ABMX. [e] M of ABMX. [f] For some signals, splitting patterns were recognizable but coupling constants could not be determined because of inadequate signal to noise ratios. [g] Ortho and meta uridine/Phe adducts were characterized as a mixture. [h] J in hertz.

Table 2. Effect of Triplet Quenchers and Radical Scavengers on the Quantum Yields of Destruction of 5-Iodouridine (IU) and Formation of Uridine (U) and Tyrosine Adduct **2** with Solutions Containing 1 mM IU and 8 mM *N*-Acetyltyrosine *N*-Ethylamide and Excitation at 325 nm Except As Noted

entry	solvent	quencher or scavenger	Φ (−IU)	Φ (U)	Φ (**2**)
1	H_2O, pH 7[a]	none	0.015 ± 0.003	0.0042 ± 0.0007	0.0081 ± 0.0013
2	H_2O, pH 7[a]	2-propanol, 10 mM	0.030 ± 0.005	0.0076 ± 0.0012	0.0078 ± 0.0012
3	H_2O, pH 7[a]	2-propanol, 100 mM	0.018 ± 0.004	0.015 ± 0.003	0.0024 ± 0.0004
4	H_2O, pH 7[a]	acetonitrile, 100 mM	0.015 ± 0.004	0.0046 ± 0.0011	0.0073 ± 0.0012
5	H_2O, pH 7[a]	acetonitrile, 1 M	0.011 ± 0.004	0.0080 ± 0.0012	0.0062 ± 0.0010
6	90% MeCN−10% water[b]	acetonitrile	0.13 ± 0.03	0.12 ± 0.03	0.011 ± 0.002
7	H_2O, pH 7[a]	potassium sorbate, 10 mM	0.020 ± 0.003	0.0022 ± 0.0003	0.0029 ± 0.0004
8	H_2O, pH 7[a]	potassium sorbate, 10 mM, + 2-propanol, 10 mM	0.027 ± 0.004	0.0031 ± 0.0005	0.0026 ± 0.0004

[a] 0.05 M phosphate buffer. [b] Excitation wavelength 330 nm.

Table 3. Effect of Triplet Quenchers and Radical Scavengers on the Quantum Yields of Destruction of 5-Iodouridine (IU) and Formation of Uridine (U) with Irradiation at 325 nm[a]

entry	quencher or scavenger	Φ (−IU)	Φ (U)
1	none	0.017 ± 0.004	0.010 ± 0.002
2	2-propanol, 10 mM	0.027 ± 0.006	0.014 ± 0.002
3	potassium sorbate, 10 mM	0.022 ± 0.006	0.0012 ± 0.0002
4	potassium sorbate, 10 mM, + 2-propanol, 10 mM	0.023 ± 0.005	0.0025 ± 0.0004

[a] Solutions contained 1 mM IU in 0.05 M pH 7 phosphate buffer.

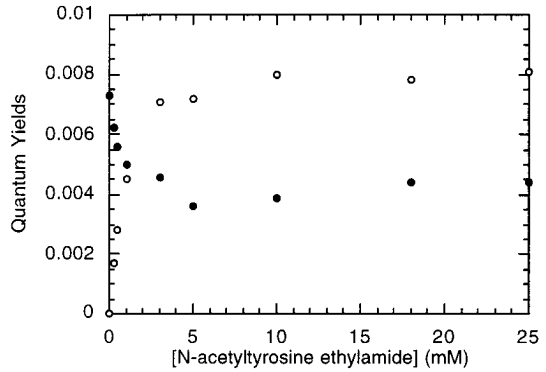

Figure 2. Observed quantum yields of formation of uridine (•) and the photoadduct **2** (○) as a function of increasing *N*-acetyltyrosine *N*-ethylamide (**1**) concentration. Solutions of 5-iodouridine (1 mM) and *N*-acetyltyrosine *N*-ethylamide in phosphate buffer (20 mM, pH 7) were irradiated at 325 nm.

increased quantum yield of U formation in this medium is also consistent with the 9% enthalpic release shortfall observed by photoacoustic calorimetry.

The role of the triplet state was explored further using three diene quenchers: *cis*-piperylene, 2,4-hexadien-1-ol, and potassium sorbate. *cis*-Piperylene was used as an effective quencher of electron-transfer-mitigated photoreduction of 5-bromouracil by 2-propanol in an earlier study.[7,8] Insignificant quenching of adduct formation was observed; however, interpretation of the experiment was complicated by the reactivity of the quenchers as π-acceptors and hydrogen atom donors toward radicals (vide infra).

Triplet reactivity of 5-iodouridine was also explored using benzophenone sensitization with excitation at 355 nm with a frequency-tripled Nd:YAG laser. As mentioned above (see Photoacoustic Calorimetry in this section), 5-iodouridine was shown to efficiently quench excited triplet benzophenone with a second-order quenching constant of 1.9×10^9 M^{-1} s^{-1} in 90% acetonitrile−10% water. The sensitized reaction of IU with **1** in the same medium gave adduct **2**, and the quantum yield was 3.1×10^{-3}, assuming that complete energy transfer took place between benzophenone and iodouridine. However, tyrosine also is known to quench benzophenone excited triplet states in 1:4 (v/v) acetonitrile−water solution with a reported quenching constant of 2.1×10^9 M^{-1} s^{-1}.[25] Assuming that this value applies under our conditions, two-thirds of the benzophenone triplets are actually quenched by the tyrosine analog and the rest by 5-iodouridine in a solution 15 mM in IU and 30 mM in **1**. If all of the reactivity occurred via the 5-iodouridine triplet state, then the cross-linking quantum yield would go up to approximately 0.01. The quantum yield of iodouridine triplet-induced cross-linking from direct irradiation is smaller than this value by a factor equal to the iodouridine intersystem crossing quantum yield, which has never been measured at room temperature; it has been predicted to be low on the basis of a low phosphorescence quantum yield in a glass at 77 K.[26] The quantum yield for adduct formation in 90% acetonitrile−10% water solution upon direct excitation is 0.011 (Table 2, entry 6). If we assume that the intersystem crossing yield lies somewhere between 0.1 and 0.01, then between about 9% and 0.9% of all cross-linked molecules formed by direct irradiation originate from the triplet state of iodouridine; thus, the triplet state reactivity of iodouridine at most comprises only a small contribution to the formation of a uridine−tyrosine adduct.

Table 4. Effect of Excitation Wavelength on the Quantum Yields of Destruction of 5-Iodouridine (IU) and Formation of Uridine (U) and Tyrosine Adduct **2** in 0.05 M pH 7 Phosphate Buffer Containing 8 mM *N*-Acetyltyrosine *N*-Ethylamide

wavelength (nm)	[IU] (mM)	Φ (−IU)	Φ (U)	Φ (**2**)
310	0.046	0.009 ± 0.003	0.008 ± 0.004	0.011 ± 0.002
320	0.20	0.014 ± 0.004	0.003 ± 0.003	0.009 ± 0.003
330	2.1	0.019 ± 0.008	0.006 ± 0.002	0.009 ± 0.002

The 5-bromouracil chromophore shows excitation wavelength dependent photoreactivity in 2-propanol solvent with predominance of C−Br bond homolysis at shorter wavelengths and predominance of intersystem crossing followed by electron transfer reactivity at longer wavelengths.[9,10] Further, reaction of BrU with **1** in an aqueous medium showed an apparent wavelength dependence when reactivity was assumed to result from excited BrU. This apparent wavelength dependence, however, appears to result from a predominance of product, resulting from excited **1**.[14] To test for a possible wavelength dependence for IU photoreactivity, which might serve as a signature for triplet state reactivity and/or reactivity of excited **1**, a tunable Nd:YAG-pumped frequency-doubled dye laser was used to irradiate solutions of 5-iodouridine and the tyrosine derivative along iodouridine's long-wavelength absorption tail at 310, 320, and 330 nm. The resulting quantum yields from these experiments are reported in Table 4. No wavelength dependence on the cross-linking quantum yield was observed within the experimental error.

(25) Battacharyya, S. N.; Das, P. K. *J. Chem. Soc., Faraday Trans. 2* **1984**, *80*, 1107.
(26) Görner, H. *J. Photochem. Photobiol., B* **1990**, *5*, 359.

Scheme 1

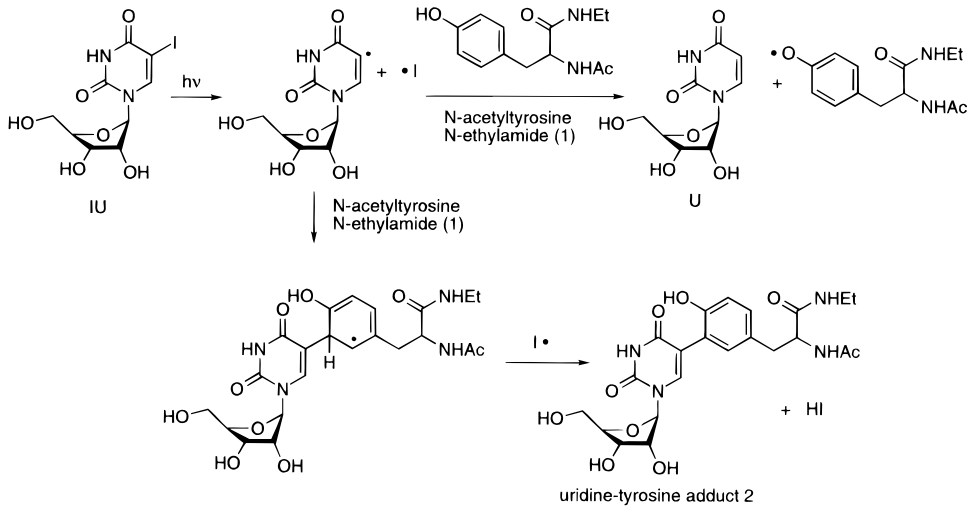

To confirm the importance of C−I bond homolysis on initiating cross-linking between iodouridine and the tyrosine derivative, a variety of hydrogen donors were tested as radical scavengers. These included 2-propanol and acetonitrile, as well as potassium sorbate and 2,4-hexadien-1-ol, which were originally intended for use as triplet quenchers. These compete with the tyrosine derivative and IU as sources of hydrogen atoms. Resulting quantum yields for all quenching experiments are shown in Table 2. In general, reasonably high concentrations of these radical scavengers were capable of significantly quenching the formation of the uridine−tyrosine adduct, suggesting that the predominance of cross-linking arises from initial C−I bond homolysis. An increase in the quantum yield of uridine formation paralleled the decrease in the quantum yield of adduct formation. Reaction via C−I bond homolysis is also consistent with quantum yield studies on 5-iodouridine in the absence of the tyrosine derivative, where approximately the same, or slightly greater, destruction quantum yield was observed as with the tyrosine present (Table 3).

The observations of insignificant quenching of uridine−tyrosine adduct **2** formation in the presence of diene triplet quencher, insignificant sensitization of cross-link formation using benzophenone, insignificant deuterium incorporation upon iodouridine photoreduction in 2-propanol-*d*, and the lack of a wavelength dependence on cross-linking efficiency led us to the conclusion that the 5-iodouridine triplet state/electron transfer mechanism makes up a minimal contribution to the photochemistry of iodouridine. Easily, less than 10% of adduct formation with *N*-acetyltyrosine *N*-ethylamide arises from this mechanism.

The most logical explanation for cross-linking with 5-iodouridine is via absorption followed by irreversible C−I bond homolysis, giving rise to a uridin-5-yl radical which undergoes radical substitution with the tyrosine derivative **1** via addition at the position ortho to the phenolic hydroxyl substituent as shown in Scheme 1. Uridine results from competitive hydrogen atom abstraction from **1**. This is borne out by the results of irradiations carried out in the presence of various radical quenchers. Of these quenchers, acetonitrile is the most unambiguous, as it is a pure hydrogen atom donor with no expected influences on triplet state or electron transfer chemistry. It is, however, only a weak hydrogen atom donor, requiring concentrations of 1 M in order to change the uridine:adduct **2** product ratio from 0.5:1 to 1.3:1. Experiments at 100 mM acetonitrile and 90% acetonitrile−10% water (v/v) give rise to results consistent with the quenching observed at 1 M acetonitrile (see Table 2).

Table 5. Relative Second-Order Rate Constants for Quenching of Uridin-5-yl Radical (U•)

reaction	$k_{relative}$
U• + tyrosine derivative **1** → adduct **2**	1.0 (defined)
U• + tyrosine derivative **1** → U	0.53
U• + 2-propanol → U	0.42
U• + acetonitrile → U	0.006
U• + sorbate → U	0.25
U• + sorbate → U−sorbate adduct?	2.3

The radical quencher 2-propanol at 10 mM concentration was found to double the quantum yield of U formation without affecting the quantum yield of adduct formation (Table 2, cf. entries 1 and 2). This contrasts somewhat with the result at 100 mM 2-propanol, where the quantum yield of U formation was 4 times higher but adduct formation was 3 times smaller (Table 2, cf. entries 1 and 3). The results of a study of photoreduction of IU in the presence of 2-propanol by Görner may provide an explanation.[17] He showed that when 2-propanol was present at even modest concentrations, photoreduction of IU occurred in part via a radical chain mechanism. The chain-propagating step was an electron transfer from 2-propanol-2-yl radical (the hydrogen-abstracted product of 2-propanol) to a ground state 5-iodouridine, giving rise to a 5-iodouridine radical anion. The radical anion then ejected iodide to generate more uridin-5-yl radical. Operation of the chain mechanism increased the quantum yield for the production of uridin-5-yl radical. In the experiment described here, the increased quantum yield of production of uridin-5-yl radical in 10 mM 2-propanol appears to cancel the decrease in the expected quantum yield of adduct formation due to radical quenching, leaving no apparent influence on the quantum yield under these conditions. 2-Propanol has been proposed to undergo electron transfer with the triplet state of 5-bromouracil,[9,10] making it potentially a more ambiguous radical quencher than acetonitrile. However, as stated above, iodouridine shows no significant triplet state or electron transfer photochemistry.

The effect of radical quenchers on the quantum yields in an aqueous medium, shown in Tables 2 and 3, is also completely consistent with products arising from C−I bond homolysis. A set of relative second-order rate constants for all radical quenching processes resulting from fitting the quantum yield data to the bond homolysis mechanism are given in Table 5. From quantum yields of U and adduct **2** formation, the quantum yield of iodouridine homolysis appears to range from 1.2% in the presence of tyrosine derivative **1** to up to 1.7% upon addition of 100 mM 2-propanol, with the increase due to the phenomenon

explained above. With sorbate present, additional products, assumed to be sorbate adducts, replace U and adduct **2** without a significant change in the quantum yield of destruction.

A predominance of acetonitrile in the medium appears to have an additional effect on uridin-5-yl radical production, with a quantum yield of 1.4% at 1 M acetonitrile, and continuing beyond 10% at 90% acetonitrile−10% water (v/v) (Table 2, entry 6). The results of a recent study of diarylmethyl chloride photochemistry by Peters and co-workers suggests a rationale for the inefficiency of C−I bond homolysis in an aqueous medium versus acetonitrile medium.[27] They observed decay of an initially formed diarylmethyl−chlorine geminate radical pair to the ground state surface by electron transfer in competition with radical cage escape. Partitioning between re-formation of starting material and a contact ion pair then occurred. Possibly, an aqueous medium facilitates electron transfer decay within the uridinyl−iodine geminate radical pair to the ground state surface in competition with radical cage escape. On the ground state surface, re-formation of starting material must be favored over formation of a contact ion pair since products from an ionic intermediate are not apparent.

Relevance to Nucleoprotein Photo-Cross-Linking. The model cross-linking reaction, which requires diffusion, appears different from the macromolecular cross-linking reaction. The results with the model study suggest that about one-third of all iodouridines should undergo photoreduction, while two-thirds will undergo cross-linking. In some macromolecular systems, cross-linking yields of a 5-iodouracil base to a tyrosine residue can exceed 90%. Why does such a discrepancy exist between the model experiments and macromolecular experiments? Orientational limitations in some nucleoprotein complexes may highly favor cross-linking over reduction. However, a more elaborate explanation seems necessary to account for the following observations. First, the irradiation time needed to achieve high-yield nucleoprotein cross-linking varies substantially as a function of the nucleoprotein complex, and we assume that irradiation time bears some resemblance to quantum yield. Second, a photoSELEX experiment starting with a combinatorial library of 10^{14} sequences bearing multiple IUs converged to a few sequences which bound with high affinity and photo-cross-linked in good yield to HIV-1 Rev protein.[7] Such convergence requires high-yield cross-linking with the iodouracil chromophore in a favorable photo-cross-linking environment and photostability with the iodouracil chromophore in an unfavorable photo-cross-linking environment. Possibly, a particular orientation of the cross-linking groups promotes an additional mechanism. In the two examples of nucleoprotein photo-cross-linking using the iodouracil chromophore in which X-ray cocrystal data are available, the iodouracil of the nucleic acid and the aromatic ring of the amino acid residue of the protein are located in a π-stacking arrangement.[28,29] Excitation of the iodouracil chromophore with an electron donor amino acid residue nearby or possibly direct excitation of an iodouracil−amino acid π-complex within a nucleoprotein complex may result in electron transfer to form a radical ion pair. High-yield cross-linking could then result from reaction of the radical ion pair via bond formation followed by loss of HI or ejection of iodide and subsequent bond formation via radical combination. Such a mechanism could have a quantum yield more than 10 times higher than the 1.5% quantum yield for simple C−I bond homolysis depending upon the specific nature of the π-complex. Although the model study with IU and **1** could not address reactivity in a π-complex, it did establish the mode and level of reactivity of the iodouracil chromophore in a non-π-stacking environment.

Concluding Remarks. Electronically excited 5-iodouridine reacts in an aqueous medium with *N*-acetyltyrosine *N*-ethylamide (**1**) to yield uridine and adduct **2** in a 1:2 mole ratio and with *N*-acetylphenylalanine to yield uridine and three regioisomeric adducts, **3o**, **3m**, and **3p**, also in a 1:2 mole ratio. Product studies, photoacoustic calorimetric measurements, deuterium labeling experiments, quantum yield measurements, and radical quenching studies together indicate that photoreduction and adduct formation are initiated by irreversible carbon−iodine bond homolysis in the singlet state followed by hydrogen atom abstraction from **1** and radical addition to **1**, respectively.

Experimental Section

General Remarks. 5-Iodouracil and 5-iodouridine (Sigma), as well as ferrocene, 2-propanol-*d*, potassium chromate, and potassium phosphate buffer (Aldrich), were used as received without further purification. *N*-Acetyltyrosine *N*-ethylamide was synthesized from *N*-acetyltyrosine as previously described[9] and recrystallized in ethyl acetate before use. Methanol and acetonitrile (HPLC grade, Burdick and Jackson) and water (Millipore, 18 MΩ cm) were used as received. ^{1}H NMR data were collected with a Bruker AM-400 spectrometer operating at 400 MHz and UV−vis spectra with a Hewlett-Packard 8452A spectrometer. HPLC analyses were performed with a Hewlett-Packard 1090 chromatograph equipped with a UV−vis diode array detector and a Hewlett-Packard 5 μm, C-18 reversed phase, microbore column (2.1 mm × 10 cm). Detection was typically carried out at 280 nm with a 60 nm bandwidth. Mixtures of methanol and either water or 0.001 M pH 6.8, phosphate buffer were used as eluents.

Emission Spectroscopy. Fluorescence quantum yields were measured with an apparatus consisting of a 1 kW xenon arc lamp, a SPEX 1320 0.5 m double excitation monochromator with 1.5 mm slits, a SPEX 1702 0.75 m emission monochromator with 1.5 mm slits, a Centronic Series 4283 Model S25 photomultiplier tube housed in a Bailey Instruments CHA-1 air-cooled housing, and SPEX digital single photon counting electronics interfaced to an IBM-compatible computer. Emitted light was typically collected at a 14° angle relative to the incident light. 9,10-Diphenylanthracene (Aldrich, Gold Label) dissolved in *n*-pentane (Aldrich) was used as the fluorescence standard.

Photoacoustic Calorimetry. The apparatus for photoacoustic calorimetry has been previously described.[30] Briefly, a cuvette equipped with a stainless-steel-encased PZT (lead zirconate−lead titanate) acoustic sensor (0.5 MHz resonance frequency) clamped to its side in acoustic contact was irradiated at right angles to the sensor with a nanosecond laser. The laser sources used was a PRA LN1000/102 nitrogen-pumped dye laser (Exciton BPBD dye, emission maximum at 365 nm, 1.5 Hz repetition rate, 0.5 ns pulse width), a Lambda-Physik EMG-101 XeCl excimer laser (308 nm, 2−10 Hz repetition rate, 10 ns pulse width), or a Spectra Physics DCR/PDL frequency-doubled Nd:YAG-pumped dye laser (Exciton DCM dye, tunable output from 310 to 330 nm, 10 Hz, 4 ns pulse width). A Gould 4072 digital storage oscilloscope was used to record the acoustic waveforms at 10 ns per point, which were stored on an IBM PC. Laser Precision Rj-7000 pyrolytic energy probes were used to monitor both the laser energy and the transmittance of the solutions to the excitation beam. Typically, 100 laser shots were averaged in cases where the solutions were not stirred, while 20 shots were averaged in cases where a microflea stir bar was used to briefly stir the solution in between individual laser shots. A negligible difference was found in the results with and without stirring.

The data analysis for photoacoustic calorimetry has been described previously.[31] An iterative nonlinear least squares procedure was used

(27) Lipson, M.; Deniz, A. A.; Peters, K. S. *J. Phys. Chem.* **1996**, *100*, 3580.
(28) Valegard, K., Murray, J. B., Stockley, P. G., Stonehouse, N. J.; Liljas, L. *Nature* **1994**, *371*, 623.
(29) Oubridge, C.; Ito, N.; Evans, P. R.; Teo, C. H.; Nagai, K. *Nature* **1994**, *372*, 432.
(30) Peters, K. S.; Snyder, G. J. *Science* **1988**, *241*, 1053.
(31) Norris, C. L.; Peters, K. S. *Biophys. J.* **1993**, *65*, 1660.

to determine the best fit parameters for amplitude factors and rate constants (if applicable). Ferrocene was used as the calibration compound in organic solvents, while potassium chromate was used in aqueous solution.

Photoreduction of 5-Iodouridine in 2-Propanol-*d*. 5-Iodouridine (13.5 mg, 0.036 mmol) was dissolved in 2 mL of D_2O to exchange acidic protons for deuterons. The D_2O was removed in vacuo, and the solid contents were dissolved in 5 mL of 2-propanol-*d*. A 1.5 mL aliquot was transferred to a quartz cuvette and irradiated with a Lambda Physik EMG-101 XeCl excimer laser (308 nm, 10 Hz, 40 mJ/pulse) for 35 min. Approximately 50% of the 5-iodouridine was reduced to uridine as indicated by analytical reversed phase HPLC. The solvent was removed in vacuo, and the resulting crude yellow solid was analyzed by ^{1}H NMR spectroscopy in D_2O. No detectable deuterium incorporation was apparent at the 5-position of the uridine.

Photoreaction of 5-Iodouridine with *N*-Acetyltyrosine *N*-Ethylamide. 5-Iodouridine (111 mg, 0.3 mmol) and *N*-acetyltyrosine *N*-ethyl amide (325 mg, 1.3 mmol) were added to a 100 mL volumetric flask and diluted to the mark with ultra pure water. The homogeneous solution was transferred to a 100 mL quartz photocell bearing a magnetic stirbar. The solution was degassed for 15 min with argon and irradiated with stirring and continuous argon flow at 10 °C for 7 h with 308 nm monochromatic light (XeCl, 90 mJ/pulse, 10 Hz). The yield of *N*-acetyl-*m*-(5-uridinyl)tyrosine *N*-ethylamide (**2**) as determined by analytical HPLC was 30% (60% after correction for recovered starting material). Adduct **3** was isolated by preparative reversed phase HPLC on a Rainin 100 Å spherical pore C18 column, 10 mm × 25 cm, eluting with a methanol−water gradient (100% H_2O to 100% MeOH in 30 min at 4.3 mL/min). Solvent was removed in vacuo to give a white solid: mp 175−178 °C; UV (H_2O) λ_{max} 270 nm, ϵ_{280} = 6970, ϵ_{308} = 2480, ϵ_{325} = 752 L mol^{-1} cm^{-1}; mass spectrum (FAB$^-$) *m*/*z* 491, (FAB$^+$) *m*/*z* 493 (calculated M + 1, 493), exact mass 493.1935 (calculated M + 1, 493.1934); ^{1}H NMR, Table 1; ^{1}H NOE difference spectrum, irradiation at the resonance frequency for the proton at C6 gave a 2% enhancement of the resonance signal for the proton at *o*′ and 0% enhancement of the signal for the protons at the *β*-position (see the structure associated with Table 1 for the numbering scheme).

Photoreaction of 5-Iodouridine with *N*-Acetylphenylalanine *N*-Ethylamide. 5-Iodouridine (110 mg, 0.3 mmol) and *N*-acetylphenylalanine *N*-ethyl amide (304 mg, 1.3 mmol) were added to a 100 mL volumetric flask and diluted to the mark with ultrapure water. The homogeneous solution was transferred to a 100 mL quartz photocell bearing a magnetic stirbar. The solution was degassed for 15 min with argon and irradiated with stirring and continuous argon flow at 4 °C for 4 h with 308 nm monochromatic light (XeCl, 90 mJ/pulse, 10 Hz). HPLC analysis showed less than 5% IU, 30% U, and the balance as a mixture of the ortho, meta, and para *N*-acetyl(5-uridinyl)phenylalanine *N*-ethylamides, **3o**, **3m**, and **3p**, in the ratio 1:2:1. The adducts were isolated in a combined yield of 15% by preparative reversed phase HPLC as described above for the isolation of **2**. The ortho and meta adducts coeluted as a 1:2 molar mixture and were analyzed without further separation. Solvent was removed in vacuo to give a white solid: mass spectrum for all three adducts (FAB$^-$) *m*/*z* 475, (FAB$^+$) *m*/*z* 477 (calculated for M + 1, 477); ^{1}H NMR, Table 1.

Quantum Yield Measurements. Laser light was utilized for all quantum yield measurements. For light at 308 nm, either the Lambda Physik excimer laser described above or an MPB PSX-100 XeCl excimer laser (10−100 Hz repetition rate, 2.5 ns/pulse) was used. Light at 325 nm was obtained from an Omnichrome Series 74 continuous-wave HeCd laser. For wavelength dependence studies, the same Nd:YAG-pumped frequency-doubled dye laser described above (see Experimental: Photoacoustic Calorimetry in this section) was used to obtain light from 310 to 330 nm. To obtain laser light for the benzophenone sensitization quantum yield measurements at 355 nm, the Spectra-Physics DCR Nd:YAG laser, used to pump the PDL dye laser, was used alone, and the output was frequency-tripled.

Actinometry was carried out using either a Scientech 362 power meter or two Laser Precision Rj-7000 pyrolytic energy probes arranged in a transmission/reflection orientation relative to a beam splitter. With the energy probe orientation, absorbances to the laser light could be monitored during the experiment. Screw top-sealed Spectrocell SUV cuvettes were used and were degassed in most cases by bubbling prepurified argon for at least 5 min through a 1 mL solution of starting materials. Because the absorbances during most irradiations tended to increase as the starting material was destroyed due to product absorption, most irradiations were carried out to <15% destruction of the limiting reagent, which was usually the iodouridine. The iodouridine absorbance versus time plot assumed a linear decay of iodouridine in order to subtract out the absorption caused by the photoproducts. The power absorbed by the iodouridine was then calculated for each absorbance-monitoring time point, and this power was then trapezoid-rule-integrated to determine the total energy absorbed by the iodouridine. For experiments with the Nd:YAG-pumped dye laser, which suffered from severe power drift and a need for constant retuning, a computer program written in C was employed to make the actinometry calculation. Due to the variability in the calibration of the power or energy meters as well as the number of assumptions made in subtracting out non-starting-material absorption, the typical actinometry error was estimated conservatively at 15%. Quantification of reactant depletion and product buildup was followed by HPLC at 280 nm.

Quantum Yields of Formation of Uridine and Adduct 2 as a Function of *N*-Acetyltyrosine *N*-Ethylamide Concentration. 5-Iodouridine (18.9 mg, 0.050 mmol) was diluted to 25 mL in phosphate buffer (20 mM, pH 7) to give a 2 mM stock 2× solution. *N*-Acetyltyrosine *N*-ethylamide (25 mg, 0.10 mmol) was diluted to 2.0 mL in phosphate buffer to give a 50 mM stock solution. The tyrosine stock solution was serially diluted to afford 50, 36, 20, 10, 6, 2, 1, 0.5, and 0 mM tyrosine 2× solutions. Individual reaction samples were prepared by mixing 0.5 mL of iodouridine 2× stock solution with 0.5 mL of the appropriate tyrosine 2× stock solution. A 750 uL aliquot of each sample was irradiated in a quartz cuvette for 4 min with a HeCd laser (325 nm, 0.0395 W). Light absorbance ($A \approx 0.016$) was monitored by UV spectroscopy. Irradiated samples were analyzed by reversed phase analytical HPLC.

Acknowledgment. We thank the Council for Tobacco Research, the National Science Foundation, the RNA Center at the University of Colorado, and Nexstar Pharmaceuticals, Inc., for financial assistance. T.H.K. also thanks the University of Colorado Council on Research and Creative Work for a Faculty Fellowship. We thank Mary Kasparian for assistance with some initial photoacoustic calorimetric experiments, Steve Leone for the use of a dye laser, Kevin Peters for the use of a Nd:YAG laser and photoacoustic calorimeter, Josef Michl for the use of fluorescence equipment, and Marc Schottelius for help with the fluorescence quantum yield measurements.

JA9607852